THE JOURNAL OF PHYSICAL CHEMISTRY C
A JOURNAL OF THE AMERICAN CHEMICAL SOCIETY

pubs.acs.org/JPCC

Article

Proximity Effect on the Reactivity of Dioxygen Activated over Distant Binuclear Fe Sites in Zeolite Matrices

Stepan Sklenak,* Thomas Groizard, Hana Jirglova, Petr Sazama, and Jiri Dedecek

Cite This: J. Phys. Chem. C 2022, 126, 4854−4861

Read Online

ACCESS | Metrics & More | Article Recommendations

ABSTRACT: Distant binuclear cationic M(II) centers in transition-metal-exchanged zeolites were shown to activate dioxygen by its splitting at room temperature to form a pair of very active oxygen species (i.e., α-oxygens) able to subsequently oxidize methane to methanol at room temperature. Selective oxidations of methane and other hydrocarbons are of extreme importance because of their potential for the transformation of hydrocarbons to valuable products. The reactivity of the α-oxygens with dihydrogen was investigated to obtain insight into the reactivity of these unique species. The reduction of Fe(IV)═O centers of pairs of distant α-oxygen atoms is a model reaction that allows for the study of the effect of the proximity of the other Fe(IV)═O site on the reactivity of the α-oxygen. The reduction by dihydrogen is also the key reaction for the quantification of these unique sites by temperature-programmed reduction (TPR) techniques. Our study reveals that (i) there is no direct concurrent reaction of both the Fe(IV)═O centers of pairs of the distant α-oxygen atoms with a molecule of dihydrogen; (ii) first, one Fe(IV)═O site of a pair of the distant α-oxygen atoms reacts with H_2(g) to form a water molecule, which is adsorbed on the Fe(II) cation while the other Fe(IV)═O site is intact. Afterward, one of the two H atoms of the adsorbed water molecule migrates to yield two Fe(III)OH groups, which subsequently react with another molecule of dihydrogen to give two water molecules, each adsorbed on one Fe(II) cation; (iii) an isolated Fe(IV)═O site is reduced by the same mechanism as the first Fe(IV)═O site of a pair of the distant α-oxygen atoms to yield H_2O adsorbed on the Fe(II) cation; and (iv) lower reducibility of the Fe(IV)═O centers of pairs of the distant α-oxygen atoms with respect to the isolated Fe(IV)═O sites.

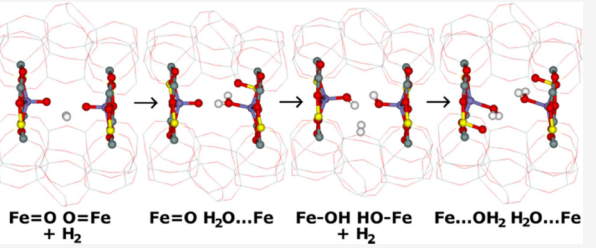

1. INTRODUCTION

Zeolites are crystalline microporous aluminosilicates widely used as ion exchangers, adsorbents, and catalysts in industrial chemical processes. Their transition-metal-exchanged forms were discovered as exceptional redox catalysts.[1,2] Panov et al. discovered α-oxygen atoms with unique reactivity formed on a divalent iron-exchanged ZSM-5 zeolite.[3,4] This α-oxygen on Fe is defined as the active oxygen species created by the N_2O oxidation of Fe and capable of oxidizing H_2, CO,[3] benzene,[5,6] and methane[3,7] at room temperature. The structure of the α-oxygen on Fe was suggested to be a $[Fe(IV)═O]^{2+}$ species, which is balanced by the negative charges of two AlO_4^- tetrahedra located in the ring of the zeolite framework that creates an extra-framework cationic site for divalent cations.[8,9] Tabor et al. have freshly identified that equally highly active α-oxygen capable of selectively oxidizing methane to methanol at room temperature can be prepared not only on Fe(II)-zeolites but also on zeolites exchanged with other divalent transition-metal cations. The α-oxygen is formed over Co(II)-ferrierite and Ni(II)-ferrierite by the abstraction of the oxygen atom from N_2O by pairs of distant binuclear transition metal M(II) (M = Co and Ni) cations.[10]

Very recently, Tabor et al. have observed the formation of very active oxygen Fe(IV)═O species from O_2 at room temperature by a pair of distant binuclear Fe(II) centers stabilized in the matrix of the ferrierite zeolite.[11] This delicately designed binuclear Fe(II) site converts methane into methanol at room temperature using O_2 as the oxidant, representing a breakthrough in methane oxidation catalysis.[12] In addition, Tabor et al. have newly showed that the distant binuclear Fe(II) sites with suitable structural parameters accommodated in various zeolites can split dioxygen and form a pair of distant Fe(IV)═O sites.[11,13] Moreover, dioxygen activation (i.e., the formation of a pair of distant M(IV)═O) has been achieved over distant binuclear M(II) centers (M = Ni, Mn, and Co) accommodated in the framework of the ferrierite zeolite.[14,15] These pairs of distant M(IV)═O species can oxidize methane to methanol at room temperature.[15] Therefore, the ability to cleave dioxygen to yield a pair of distant very active oxygen M(IV)═O (M = Fe, Ni, Mn, and Co) species represents a

Received: December 23, 2021
Revised: February 13, 2022
Published: March 7, 2022

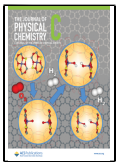

https://doi.org/10.1021/acs.jpcc.1c10821
J. Phys. Chem. C 2022, 126, 4854−4861

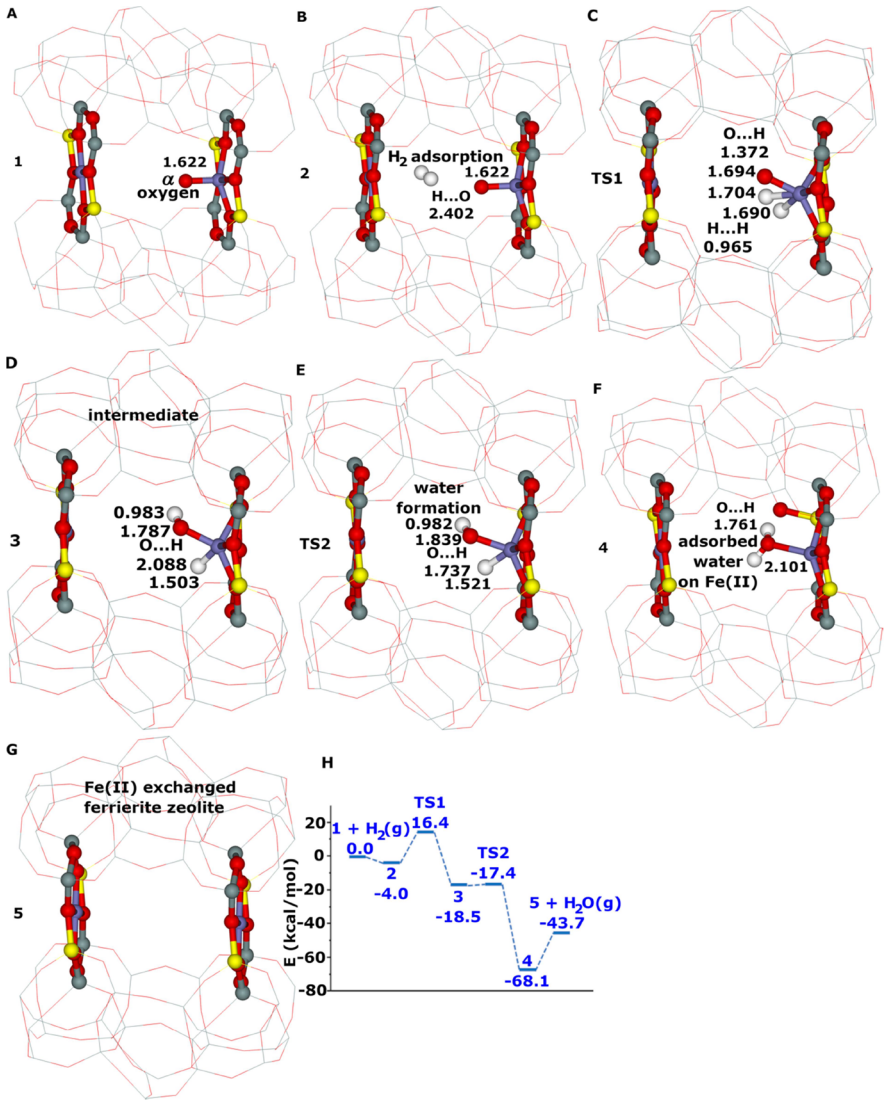

Figure 1. Reduction of the [Fe O═Fe] complex **1** by H_2(g). Optimized structures for the (A) [Fe O═Fe] complex **1** (S = 8/2) featuring the isolated α-oxygen atom, (B) [Fe H_2...O═Fe] complex **2** (S = 8/2), (C) transition state **TS1** (S = 8/2), (D) [Fe (H)HO−Fe] complex **3** (S = 8/2), (E) transition state **TS2** (S = 8/2), (F) [Fe H_2O...Fe] complex **4** (S = 8/2), (G) [Fe Fe] complex **5** (S = 8/2) possessing two bare Fe(II) cations. The distances are in Å. Silicon atoms are in gray, oxygen atoms are in red, aluminum atoms are in yellow, and iron atoms are in blue. Schematic energy profile (in kilocalorie per mol) for the spin state S = 8/2 (blue profile) for (H) the reduction of the [Fe O═Fe] complex **1** by H_2(g) to give the [Fe Fe] complex **5**.

general property of the distant binuclear M(II) centers stabilized in various aluminosilicate matrices and (i) capable of the M(II) → M(IV) redox cycle and (ii) possessing appropriate structural parameters. These findings suggest the possibility of developing M-zeolite-based systems for the dioxygen activation for direct oxidations using various transition-metal cations and different zeolites.

The distant binuclear M(II) sites represent very new catalytic centers, and therefore, our knowledge regarding (i) their behavior and (ii) the reactivity of pairs of distant M(IV)═O is greatly limited. Nevertheless, the limited space of the ferrierite cavity with two M(IV)═O species, and especially, the very short distance between the two α-oxygen atoms suggest that steric hindrance together with a possible cooperation of both the M(IV)═O species can affect the reactivity of pairs of distant M(IV)═O. Therefore, the transfer of knowledge regarding the reactivity of isolated Fe(IV)═O sites prepared by the oxidation of isolated Fe(II) cations by N_2O obtained during three decades is very limited and cannot be used for the prediction of the reactivity of pairs of distant M(IV)═O centers. Therefore, detailed investigations concerning the reactivity of pairs of distant M(IV)═O sites are highly desirable.

In this article, we use periodic density functional theory (DFT) calculations to investigate, for the first time, the detailed mechanism of the reduction of Fe(IV)═O by dihydrogen. The findings attained for the Fe(IV)═O centers of pairs of the distant α-oxygen atoms are compared with those obtained for the isolated Fe(IV)═O sites. The iron(II)-exchanged ferrierite zeolite was chosen for this examination as the most studied representative of the systems with distant binuclear M(II) sites able to activate dioxygen by a new mechanism: a direct dissociation followed by the formation of a pair of the distant α-oxygen atoms.[11,13−15] The oxidation of dihydrogen, which is the simplest oxidation reaction, was chosen for comparison of the activity of both the types of

https://doi.org/10.1021/acs.jpcc.1c10821
J. Phys. Chem. C 2022, 126, 4854−4861

Fe(IV)=O. Moreover, the reduction of Fe(IV)=O by dihydrogen represents the basis of the H_2-TPR (temperature-programmed reduction by dihydrogen) method, which is one of the essential methods used for the characterization of cationic species in zeolites. It should be noted that H_2-TPR can play a significant role in investigations of catalytic systems based on the distant binuclear cationic sites (e.g., for the selective oxidation of methane) because hitherto spectroscopic methods for the quantitative analysis of M(IV)=O sites have not yet been reported. The achieved results reveal that (i) one Fe(IV)=O site of a pair of the distant α-oxygen atoms as well as (ii) an isolated Fe(IV)=O site reacts with H_2(g) to yield a water molecule that is adsorbed on the Fe(II) cation. Subsequently, for the former system, one hydrogen atom from the adsorbed water molecule is abstracted by the other α-oxygen atom to give two Fe(III)−OH groups which are afterward reduced by another H_2(g) to form two H_2O adsorbed on the two Fe(II) cations. Conversely, for the latter system, the reaction is finished.

2. COMPUTATIONAL DETAILS

2.1. Structural Models. The calculations were performed for a model with two Fe(II) cations accommodated in two adjacent β2 sites[8,10,11,13,14,16−18] of ferrierite. The model has a P1 symmetry and features a supercell composed of two-unit cells along the c dimension (i.e., a = 18.651, b = 14.173, and c = 14.808 Å). The model contains four Al/Si substitutions forming two adjacent β2 sites with the four Al atoms located in the T2 sites of the two adjacent six-rings [only the β2 site with both Al in T2 was found in the ferrierite framework of this ferrierite zeolite[16]], accommodating two Fe(II) cations. The model was identical to those used in our prior studies.[10,11]

2.2. Electronic Structure Calculations. Periodic DFT calculations were carried out using the Vienna Ab initio Simulation Package (VASP) code.[19−22] The high-spin electron configurations[8,11,17,23,24] $d^5\uparrow\ d^1\downarrow$ of Fe(II), $d^5\uparrow\ d^0\downarrow$ of Fe(III), $d^4\uparrow\ d^0\downarrow$ of Fe(IV), and other possible spin states were employed for the Fe species for all the minima and transition states to localize the electronic ground state for all the species. Moreover, for all the calculated optimized structures, the electron configuration used was verified that it really corresponds to the ground state. The Kohn−Sham equations were solved variationally in a plane-wave basis set using the projector-augmented wave method of Blöchl,[25] as adapted by Kresse and Joubert.[26] The exchange-correlation energy was described by the Perdew−Burke−Ernzerhof[27] (PBE) generalized gradient approximation (GGA) functional. Brillouin zone sampling was restricted to the Γ point. A plane-wave cutoff of 600 eV and the density-dependent energy correction (dDsC) dispersion correction[28,29] were used for the geometry optimizations.

2.3. Geometry Optimizations. The atomic positions were optimized by employing a conjugate−gradient algorithm minimization of energies and forces, while the lattice parameters were fixed (constant volume) at their experimental values.

3. COMPUTATIONAL RESULTS

3.1. Spin States. The high-spin configurations $d^5\uparrow\ d^1\downarrow$ of Fe(II), $d^5\uparrow\ d^0\downarrow$ of Fe(III), and $d^4\uparrow\ d^0\downarrow$ of Fe(IV) were found to be the ground electronic state for all the species calculated. Therefore, the structures with two Fe(II) or Fe(IV) cations have eight unpaired electrons. Conversely, the species with two Fe(III)-OH moieties (i.e., complexes **10′** and **11′**) possess ten unpaired electrons, and their spin variants with ten unpaired electrons are more stable than those with eight (i.e., complexes **10** and **11**). Spin-state changes throughout the course of the reaction for systems containing transition metals are quite common.[30]

3.2. Mechanisms of the Reduction of α-Oxygen Atoms by H_2(g). Three reaction mechanisms are reported. The first one describes the reduction of the isolated α-oxygen atom of a [Fe O=Fe] complex **1** (Section 3.2.1), while the second mechanism relates to the reduction of one α-oxygen atom of a pair of the distant α-oxygen atoms[11] of a [Fe=O O=Fe] complex **6** (Section 3.2.2). It is shown that after one of the distant α-oxygen atoms is reduced to Fe(II) and adsorbed H_2O, the adsorbed water reacts with the other α-oxygen atom to yield two Fe(III)−OH species of the [Fe−OH HO−Fe] complex **10′**. Finally, a plausible mechanism to reduce the two collaborating Fe(III)−OH species of the [Fe−OH HO−Fe] complex **10′** is revealed in Sections 3.2.3. Furthermore, our calculations also showed that there was no direct simultaneous reduction of both the α-oxygen atoms of the [Fe=O O=Fe] complex **6** to yield the [Fe−OH HO−Fe] complex **10′** as no corresponding transition state was found.

3.2.1. Reduction of the Isolated α-Oxygen Atom. Figure 1 reveals the reaction mechanism of the reduction of the isolated α-oxygen atom of the [Fe O=Fe] complex **1** by H_2(g).

The [Fe O=Fe] complex **1** (Figure 1) that features one α-oxygen atom located in two adjacent β2 cationic sites of ferrierite interacts with a molecule of dihydrogen to give a [Fe H_2...O=Fe] complex **2**. The calculations yield a small adsorption energy of 4.0 kcal/mol. The adsorbed dihydrogen molecule reacts with the α-oxygen atom to give a [Fe (H)HO−Fe] complex **3** via a transition state **TS1** (Figure 1). The formation of **3** is the rate-determining step of the entire reduction of the [Fe O=Fe] complex **1** because the corresponding calculated barrier is 20.4 kcal/mol. The related reaction energy is −14.5 kcal/mol. The complex **3** is only very short-lived as it fast rearranges via a transition state **TS2** to yield a complex **4**, which features an adsorbed water molecule on one Fe(II) cation (Figure 1). This step is very exothermic (−49.6 kcal/mol) and very facile as the barrier is tiny (1.1 kcal/mol). The water molecule formed can desorb, which costs 24.4 kcal/mol. The calculated reaction energy of the entire reaction from **1** + H_2(g) to give a complex **5** and H_2O(g) is −43.7 kcal/mol (Figure 1).

The H_2 molecule interacts with the iron atom of the Fe(IV)=O site. The H−H bond is gradually cleaved, and two O−H bonds are created. The H−H bond elongates and cleaves along the sequence **2** → **TS1** → **3** (H−H distances: 0.75, 0.97, and 2.44, respectively, Å), while two O−H bonds are formed along the two sequences—one OH: **2** → **TS1** → **3** (O−H distances: 2.40, 1.37, and 0.98, respectively, Å) and another OH: **3** → **TS2** → **4** (O−H distances: 2.09, 1.74, and 0.97, respectively, Å). Both the hydrogen atoms form elongated bonds to Fe (Fe−H distances: 1.69−1.70 Å) in **TS1**. One of them is preserved in the complex **3** (Fe−H bond distance: 1.50 Å) while the other hydrogen yields an OH group. The remaining Fe−H bond is cleaved in the subsequent step to give the complex **4** via **TS2**. The Fe−O bond is gradually cleaved along the sequence **2** → **TS1** → **3** → **TS2** →

https://doi.org/10.1021/acs.jpcc.1c10821
J. Phys. Chem. C 2022, 126, 4854−4861

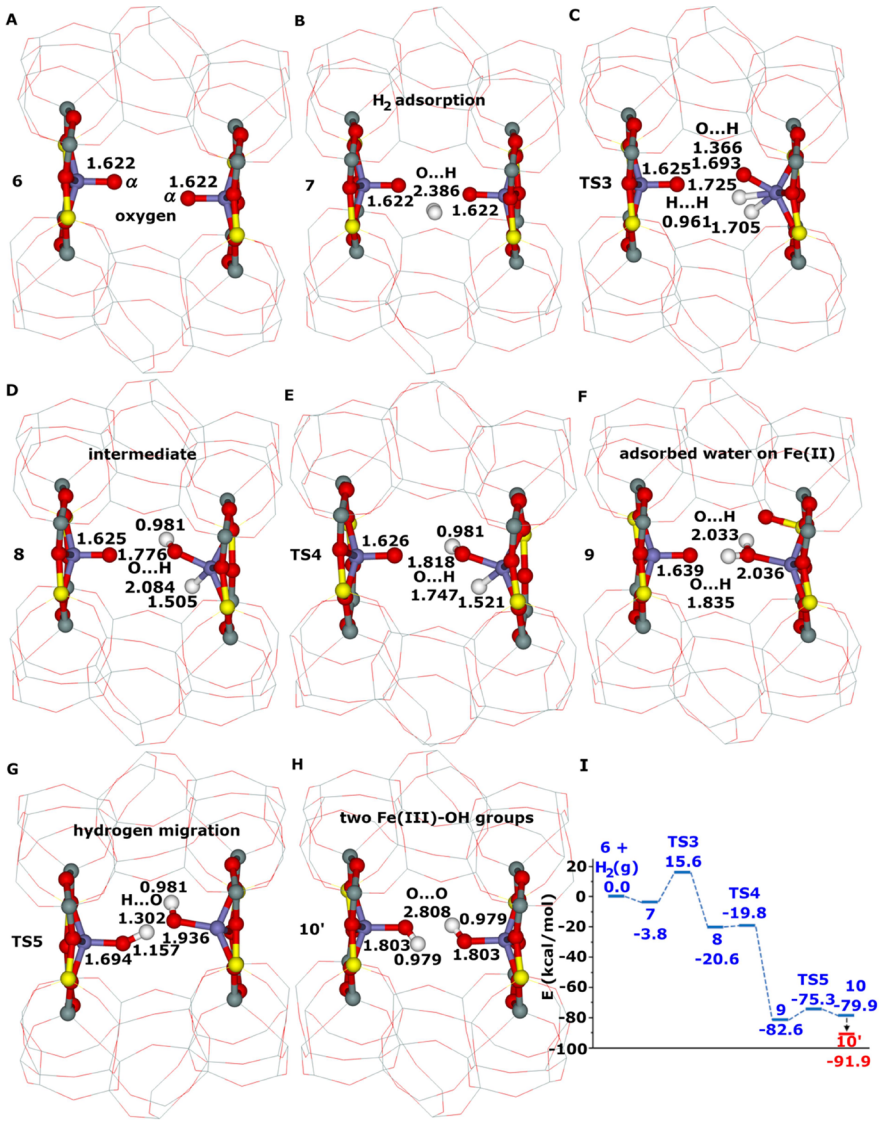

Figure 2. Reduction of the [Fe═O O═Fe] complex **6** by H_2(g). Optimized structures for the (A) [Fe═O O═Fe] complex **6** (S = 8/2) featuring a pair of the distant α-oxygen atoms, (B) [Fe═O H_2...O═Fe] complex **7** (S = 8/2), (C) transition state **TS3** (S = 8/2), (D) [Fe═O (H)HO−Fe] complex **8** (S = 8/2), and (E) transition state **TS4** (S = 8/2), (F) [Fe═O H_2O...Fe] complex **9** (S = 8/2), and (G) transition state **TS5** (S = 8/2), (H) [Fe−OH HO−Fe] complex **10′** (S = 10/2). Distances are in Å. Silicon atoms are in gray, oxygen atoms are in red, aluminum atoms are in yellow, and iron atoms are in blue. Schematic energy profile (in kilocalorie per mol) for the spin states S = 8/2 (blue profile) and S = 10/2 (red profile) for (I) the reduction of the [Fe═O O═Fe] complex **6** by H_2(g) to yield the [Fe−OH HO−Fe] complex **10′**.

4 (Fe−O distances: 1.62, 1.69, 1.79, 1.84, 2.10, respectively, Å).

3.2.2. Reduction of One α-Oxygen Atom of a Pair of the Distant α-Oxygen Atoms. The corresponding reaction mechanism is depicted in Figure 2.

Figure 2 shows that the reaction steps of the reduction of the [Fe═O O═Fe] complex **6** by H_2(g) to yield a [Fe═O H_2O...Fe] complex **9** are the same as those calculated for the reduction of the [Fe O═Fe] complex **1** (Figure 1). **6** interacts with a molecule of dihydrogen to yield a [Fe═O H_2...O═Fe] complex **7**. The calculated adsorption energy is only 3.8 kcal/mol. The adsorbed dihydrogen molecule reacts with one of the α-oxygen atoms of a pair of the distant α-oxygen atoms to give a [Fe═O (H)HO−Fe] complex **8** via the transition state **TS3** (Figure 2). The corresponding barrier is 19.4 kcal/mol. The reaction step **7** → **8** is calculated to be exothermic by 16.8 kcal/mol. When the [Fe═O (H)HO−Fe] complex **8** is created, it swiftly rearranges, as the corresponding barrier is only 0.8 kcal/mol, via the transition state **TS4** to yield the [Fe═O H_2O...Fe] complex **9** with an adsorbed water molecule on one Fe(II) cation. The formation of the adsorbed water molecule is very exothermic (62.0 kcal/mol). Both of the hydrogen atoms of the adsorbed water molecule of the [Fe═O H_2O...Fe] complex **9** form a hydrogen bond. One to a framework O atom and the other to the α-oxygen atom (Figure 2F). The latter is therefore well-positioned to migrate to the α-oxygen atom. Therefore, the adsorbed water is only short-lived, and instead of desorbing into the gas phase (which would cost 34.9 kcal/mol), it very fast reacts via the transition state **TS5** to yield the [Fe−OH HO−Fe] complex **10** featuring two Fe(III)−OH groups. The calculated barrier of 7.3 kcal/mol is tiny. Our calculations moreover reveal that the [Fe−OH HO−Fe] complex **10** undergoes a spin cross-over to form the [Fe−OH HO−Fe] complex **10′** with ten unpaired electrons.

https://doi.org/10.1021/acs.jpcc.1c10821
J. Phys. Chem. C 2022, 126, 4854−4861

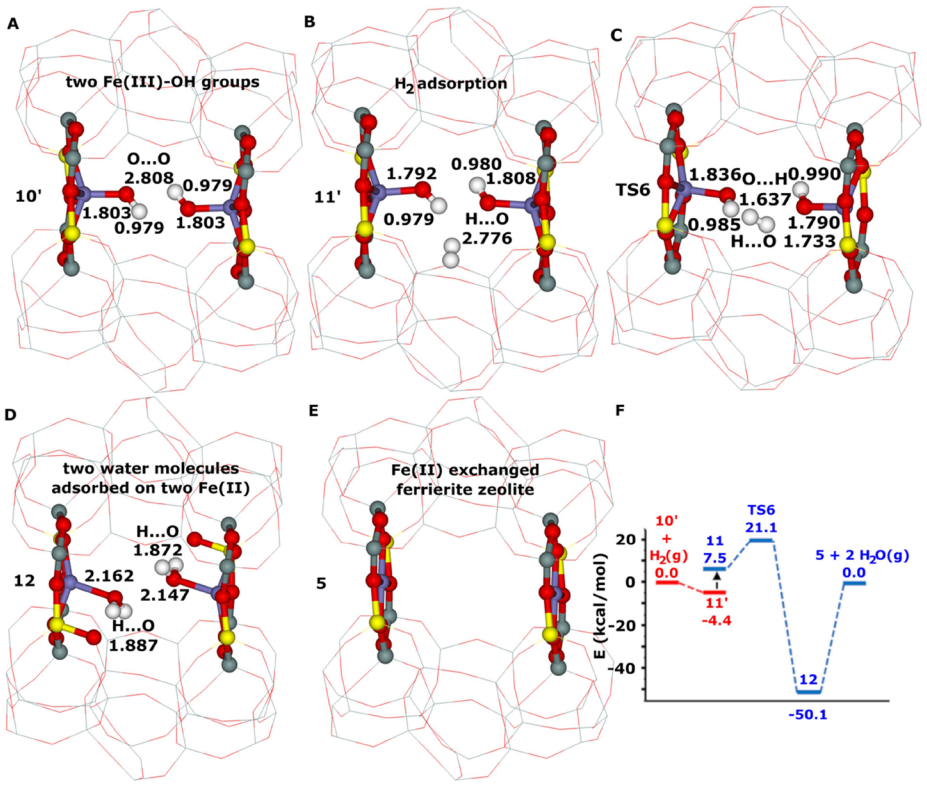

Figure 3. Reduction of the [Fe−OH HO−Fe] complex **10′** by H_2(g). Optimized structures for the (A) [Fe−OH HO−Fe] complex **10′** (S = 10/2), (B) [Fe−(H)O...H_2...O(H)−Fe] complex **11′** (S = 10/2), (C) transition state **TS6** (S = 8/2), (D) [Fe...OH_2 H_2O...Fe] complex **12** (S = 8/2), and (E) [Fe Fe] complex **5** (S = 8/2) possessing two bare Fe(II) cations. The distances are in Å. Silicon atoms are in gray, oxygen atoms are in red, aluminum atoms are in yellow, and iron atoms are in blue. Schematic energy profile (in kilocalorie per mol) for the spin states S = 8/2 (blue profile) and S = 10/2 (red profile) for (F) the reduction of the [Fe−OH HO−Fe] complex **10′** by H_2(g) to form the [Fe Fe] complex **5**.

10′ is calculated to be more stable than **10** by 12.0 kcal/mol as this species with two Fe(III) cations prefers the high-spin configurations $d^5\uparrow$ $d^0\downarrow$. The reaction step **9** → **10′** is calculated to be exothermic by 9.3 kcal/mol. Our calculations reveal that **9** is only short-lived as it fast yields **10′**, which is more stable. Also, the desorption of the water molecule to yield **1** does not occur as it costs 34.9 kcal/mol. Therefore, the reduction proceeds from the complex **10′**, not from the complex **9**.

Similarly, as in the case of the reduction of the [Fe O═Fe] complex **1** (Figure 1), the H_2 molecule reacts with Fe of one Fe(IV)═O moiety. The H−H bond is gradually cleaved, and two O−H bonds are created. The H−H bond elongates and cleaves along the sequence **7** → **TS3** → **8** (H−H distances: 0.75, 0.96, and 2.43, respectively, Å) while O−H bonds are formed along the sequences **7** → **TS3** → **8** (O−H distances: 2.39, 1.37, and 0.98, respectively, Å) and **8** → **TS4** → **9** (O−H distances: 2.08, 1.75, and 0.99, respectively, Å). Both hydrogen atoms form elongated bonds to Fe (Fe−H distances: 1.71 and 1.73 Å) in **TS3**. One of them is preserved in the complex **8** (Fe−H bond distance: 1.51 Å), while the other hydrogen yields OH. The Fe−H bond is cleaved in the subsequent step to give the complex **9** via **TS4**. The Fe−O bond is gradually cleaved along the sequences **7** → **TS3** → **8** → **TS4** → **9** (Fe−O distances: 1.62, 1.69, 1.78, 1.82, 2.04, respectively, Å).

3.2.3. Reduction of the Two Cooperating Fe(III)−OH Groups of the [Fe−OH HO−Fe] Complex 10′ via a Concerted Mechanism. Figure 3 reveals a concerted mechanism of the reduction of two cooperating Fe(III)−OH groups of the complex **10′** by H_2(g).

The two oxygen atoms of the two Fe(III)−OH groups of the complex **10′** react with H_2(g) to yield the [Fe−(H)O...H_2...O(H)−Fe] complex **11′**. The calculated adsorption energy is 4.4 kcal/mol. **11′** undergoes a spin cross-over to give **11** with eight unpaired electrons (Figure 3). The H−H bond is subsequently cleaved, and two new H−O bonds are formed via a transition state **TS6** (Figure 3) to give a [Fe...OH_2 H_2O...Fe] complex **12** featuring two adsorbed water molecules on two Fe(II) cations. The complex **12** with two Fe(II) cations prefers the high-spin configurations $d^5\uparrow$ $d^1\downarrow$. The creation of **12** is the rate-determining step of the entire reduction of the [Fe═O O═Fe] complex **6** as the calculated barrier is 25.5 kcal/mol. The formation of two adsorbed H_2O is very exothermic (50.1 kcal/mol). It costs 50.1 kcal/mol to desorb both the water molecules to yield the [Fe Fe] complex **5**.

The H−H bond is gradually cleaved along the sequence **11′** → **TS6** → **12** (H−H distances: 0.75, 0.81, and 2.55, respectively, Å), while two O−H bonds are formed along the sequence **11′** → **TS6** → **12** (O−H distances: 2.78 and 3.53, 1.64, and 1.73, and 0.98 and 0.98, respectively, Å). Both the two Fe(III)−OH groups of the [Fe−OH HO−Fe] complex **10′** are reduced to two adsorbed water molecules on the two Fe(II) in a single step.

4. DISCUSSION

Figures 1 and 2 show that dihydrogen molecules react with the Fe atom of the Fe(IV)═O species to yield an intermediate with hydride and hydroxyl groups (the complex **3** in Figure 1 and the complex **8** in Figure 2). This reaction step is the first

https://doi.org/10.1021/acs.jpcc.1c10821
J. Phys. Chem. C 2022, 126, 4854−4861

step of the reduction of both isolated Fe(IV)=O sites (Figure 1) as well as pairs of distant Fe(IV)=O centers (Figure 2). Both the complexes **3** and **8** (Figures 1 and 2, respectively) are very short-lived, and the hydrogen atom of the Fe−H moiety is abstracted by the oxygen atom of the Fe(III)−OH group to yield the adsorbed water molecules on Fe(II) (the complexes **4** and **9**, respectively). This second step is the same for both the cases. The formation of **4** is the final step of the reduction of **1**. It costs 24.4 kcal/mol to desorb the adsorbed water molecule.

The reduction of a pair of distant Fe(IV)=O centers of the complex **6** (Figure 2) does not proceed as two independent subsequent reductions of isolated Fe(IV)=O sites. When the complex **9** is formed, one hydrogen atom of the adsorbed water on Fe(II) forms a hydrogen bond to a framework O atom, while the other hydrogen atom of the adsorbed water creates a hydrogen bond to the remaining α-oxygen atom. The latter H atom is subsequently abstracted by the α-oxygen atom to yield two OH moieties of the complex **10**. **10** then undergoes a spin cross-over to give the more stable complex **10′** featuring two Fe(III)−OH groups (Figure 2). Following this, the complex **10′** reacts with another H_2(g) molecule to yield the complex **12** with two water molecules, each adsorbed on one Fe(II) cation (Figure 3). It costs 50.1 kcal/mol to desorb the two adsorbed water molecules.

The reduction of isolated Fe(IV)=O sites (Figure 1) has a different rate-determining step than the reduction of pairs of distant Fe(IV)=O centers (Figure 2). The reduction of the [Fe H_2...O=Fe] complex **2** to yield the [Fe (H)HO−Fe] complex **3** is the rate-determining step in the former case, while the reduction of the [Fe−(H)O...H_2...O(H)−Fe] complex **11′** to give the [Fe...OH_2 H_2O...Fe] complex **12** is the rate-determining step in the latter case. The corresponding calculated barriers are 20.4 and 25.5 kcal/mol, indicating a lower reducibility of the complex **6** with respect to the complex **1**.

We also investigated possibilities that H_2(g) directly reacted, without any interaction with the Fe atoms, with (i) the O atom of isolated Fe(IV)=O sites of the complex **1** to give the complex **4** (Figure 1) and (ii) both O atoms of a pair of distant Fe(IV)=O centers of the complex **6** to yield the complex **10**. However, all our attempts to locate transition states connecting the complexes **1** and **4** as well as **6** and **10** were unsuccessful.

There is an important consequence of hydrogen atom abstraction (Figure 2). When the complex **5** is oxidized by N_2O(g), the complex **1** is yielded (Figure 1). Our prior study[8] showed that the reaction was very facile. However, if the N_2O(g) used contains water, then a water molecule can adsorb on the Fe(II) cation of the complex **1** to give the complex **9** and subsequently the complex **10′** (Figure 2). It means that when water is present, then the oxidation of the ferrierite with the distant binuclear Fe(II) sites by N_2O(g) yields rather two Fe(III)−OH centers than one Fe(IV)=O site. Conversely, when the Fe-zeolite contains only isolated Fe(II) cations, they are oxidized by N_2O(g) to yield isolated Fe(IV)=O sites and the presence of water does not prevent the formation of Fe(IV)=O. This emphasizes the crucial role of both the presence of water vapor and the reaction conditions in the N_2O abatement over Fe-zeolites. Fe-zeolites (especially Fe-ferrierites) were suggested as promising materials for the N_2O abatement from nitric acid production. The very first steps of the N_2O decomposition over Fe-zeolites is the adsorption of N_2O on Fe(II) located in the active sites and the subsequent release of molecular nitrogen to form Fe(IV)=O.[8] We suggest based on our results that, on the one hand, Fe-zeolites with isolated Fe(II) centers are more suitable materials for processes at lower temperature with a significant presence of water vapor (e.g., end-of-pipe technologies). On the other hand, Fe-ferrierites with distant binuclear Fe(II) centers and with high stability resulting from the framework topology and Al distribution[31,32] represent more promising materials for processes at high temperature (thus limiting water adsorption), for which water vapor does not mean a critical issue.

The selective oxidation of methane to methanol at room temperature undoubtedly evidences the presence of the highly active α-oxygen species prepared by either splitting dioxygen[11] or the abstraction[10] of the oxygen atom from N_2O over distant binuclear Fe(II) structures. However, the quantification of the α-oxygen atoms by their reduction employing methane is accompanied by significant difficulties because the oxidation of methane to methanol may not be quantitative, and other oxidation products of methane (e.g., methoxy groups, formaldehyde, formic acid, dimethyl ether, carbon dioxide, and carbon monoxide) can be created as well depending on the reaction conditions. Moreover, some of the oxidation products can be adsorbed on the active Fe sites or other adsorption centers in the zeolite (e.g., in case of the formation of methoxy groups, extraction by water is required).[33−35] Therefore, H_2−TPR can serve as a suitable simple method for quantitative analysis of the formed α-oxygen atoms, which is essential for the development of materials for the selective oxidation of methane. The results of our DFT calculations clearly indicate that low-temperature (strictly below 0 °C) H_2−TPR has to be employed to analyze the α-oxygen atoms formed by either splitting dioxygen or the abstraction of the oxygen atom from N_2O. Moreover, in the case of the characterization of the α-oxygen atoms created from dioxygen, the presence of two bands in the H_2−TPR profile corresponding to the same α-oxygen atoms is contra-intuitively assumed. Conversely, only one band is expected to be present in the H_2−TPR profile of the α-oxygen atoms formed from N_2O.

The outcome of our study clearly evidences that even such a simple reaction as the oxidation of dihydrogen by Fe(IV)=O sites does not proceed identically for the isolated Fe(IV)=O sites and the Fe(IV)=O centers of pairs of the distant α-oxygen atoms, but there is a difference in the reaction mechanisms for these two types of centers. This finding can be most likely generalized for the M(IV)=O sites of other cations (M = Ni, Mn, and Co) as well. Moreover, the effect of the proximity of the other M(IV)=O site in the confined reaction space of the zeolite cavity will be more pronounced for reactions of bulkier molecules than dihydrogen. Thus, the reactivity of the M(IV)=O centers of pairs of the distant α-oxygen atoms formed by splitting dioxygen over distant binuclear M(II) centers cannot be predicted or interpreted based only on the knowledge gained for the isolated Fe(IV)=O sites prepared by the oxidation of isolated Fe(II) cations by N_2O obtained during three decades. Both experimental and theoretical investigations of the reactivity of the M(IV)=O centers of pairs of the distant α-oxygen atoms are highly desirable to elucidate the mechanism of the selective oxidation of methane to methanol and its release.

It should be pointed out that our computational model compares the performance of the isolated Fe(IV)=O sites and the Fe(IV)=O centers of pairs of the distant α-oxygen atoms under a condition of a low H_2(g) pressure. Moreover, the

https://doi.org/10.1021/acs.jpcc.1c10821
J. Phys. Chem. C 2022, 126, 4854−4861

model does not consider other structural effects as, for example, the presence of cations in other cationic sites and the existence of Brønsted acid sites (Si−OH−Al) in the zeolite framework, which can somewhat affect the local arrangement of the active sites and their behavior.

Panov et al. reported the selective oxidation of methane to methanol over isolated Fe(IV)=O sites in Fe-ZSM-5; however, the formed methoxy groups were strongly bound to the catalyst, and extraction by water vapor was required to release methanol from the catalyst.[4] Göltl et al. published a computational study regarding the rebound mechanism, allowing the selective oxidation of methane with the direct creation of methanol (i.e., without the formation of methoxy groups bound to the zeolite) over isolated Fe(IV)=O sites in the zeolite of the chabazite structure in 2016.[36] Tabor et al. observed this direct formation of methanol over isolated Fe(IV)=O centers in Fe−ferrierite for the first time in 2019.[10] Snyder et al. confirmed the direct methanol creation over the isolated Fe(IV)=O site for Fe-chabazite in 2021.[37] Furthermore, they showed that the size of the ring separating the individual zeolite cavities with Fe(IV)=O and potentially hindering the migration of the formed methyl radical in the zeolite channel system is the key parameter controlling the reaction pathway of the selective oxidation of methane over isolated Fe(IV)=O sites in zeolites. However, the calculated mechanism of dihydrogen oxidation over the Fe(IV)=O centers of pairs of the distant α-oxygen atoms (Figure 2) reveals that one of the hydrogen atoms of the formed adsorbed water of **9** is abstracted by the other α-oxygen atom to yield two Fe(III)−OH groups of **10′**. Analogously, a hydrogen atom abstraction can be suggested also for methanol adsorbed on a Fe(II) cation. However, this would contradict the experimentally proven direct methanol formation and desorption from the active site represented by the M(IV)=O centers of pairs of the distant α-oxygen atoms in M-ferrierites.[10,11,15] Therefore, it is evident that our current knowledge concerning the performance of isolated Fe(IV)=O sites in the selective oxidation of methane cannot represent a suitable base for the explanation of such an important reaction as the selective oxidation of methane over the M(IV)=O centers of pairs of the distant α-oxygen atoms prepared by splitting dioxygen over distant binuclear M(II) centers, but detailed studies in this field are highly desirable.

5. CONCLUSIONS

Distant binuclear cationic M(II) (M = Fe, Ni, Mn, and Co) centers in M(II)-zeolites can cleave dioxygen at room temperature to create a pair of the very active α-oxygen species (i.e., Me(IV)=O) that can subsequently oxidize methane to methanol at room temperature. The reduction by H_2(g) of (i) the Fe(IV)=O sites of a pair of the distant α-oxygen atoms and (ii) isolated Fe(IV)=O moieties in the iron(II)-exchanged ferrierite zeolite was investigated by periodic DFT calculations. Our study reveals that (i) there is no direct simultaneous reduction of both the Fe(IV)=O centers of pairs of the distant α-oxygen atoms, (ii) one Fe(IV)=O site of a pair of the distant α-oxygen atoms is reduced by a molecule of dihydrogen to yield adsorbed water on the Fe(II) cation while the other Fe(IV)=O site is intact, and subsequently, one of the hydrogen atoms of the adsorbed water is abstracted by the other α-oxygen atom to yield two Fe(III)−OH groups, which are afterward reduced by another molecule of dihydrogen to give two water molecules each adsorbed on one Fe(II) cation, (iii) an isolated Fe(IV)=O site is reduced by the same mechanism as one Fe(IV)=O site of a pair of the distant α-oxygen atoms, and (iv) lower reducibility of the Fe(IV)=O centers of pairs of the distant α-oxygen atoms relative to the isolated Fe(IV)=O sites. The obtained results clearly evidence (and most likely can be generalized for other molecules than dihydrogen as well) that the proximity of the other Fe(IV)=O site in the confined reaction space of the zeolite cavity can dramatically change the behavior of both the cooperating α-oxygen atoms and the reaction mechanism over Fe(IV)=O sites of a pair of the distant α-oxygen atoms can differ from that over isolated Fe(IV)=O sites.

AUTHOR INFORMATION

Corresponding Author

Stepan Sklenak − *J. Heyrovský Institute of Physical Chemistry of the Czech Academy of Sciences, 182 23 Prague 8, Czech Republic*; orcid.org/0000-0003-4862-857X; Email: stepan.sklenak@jh-inst.cas.cz

Authors

Thomas Groizard − *J. Heyrovský Institute of Physical Chemistry of the Czech Academy of Sciences, 182 23 Prague 8, Czech Republic*

Hana Jirglova − *J. Heyrovský Institute of Physical Chemistry of the Czech Academy of Sciences, 182 23 Prague 8, Czech Republic*

Petr Sazama − *J. Heyrovský Institute of Physical Chemistry of the Czech Academy of Sciences, 182 23 Prague 8, Czech Republic*; orcid.org/0000-0001-7795-2681

Jiri Dedecek − *J. Heyrovský Institute of Physical Chemistry of the Czech Academy of Sciences, 182 23 Prague 8, Czech Republic*

Complete contact information is available at: https://pubs.acs.org/10.1021/acs.jpcc.1c10821

Notes

The authors declare no competing financial interest.

ACKNOWLEDGMENTS

This work was supported by the Grant Agency of the Czech Republic under project # 19-02901S and # 21-45567L (2020/39/I/ST4/02559) and project RVO: 61388955. This work was supported by the Ministry of Education, Youth and Sports of the Czech Republic through the e-INFRA CZ (ID:90140).

REFERENCES

(1) Traa, Y.; Burger, B.; Weitkamp, J. Zeolite-based materials for the selective catalytic reduction of NO_x with hydrocarbons. *Microporous Mesoporous Mater.* **1999**, *30*, 3−41.

(2) Wichtelová, B.; Sobalík, Z.; Dědeček, J. Redox catalysis over metallo-zeolites: Contribution to environmental catalysis. *Appl. Catal., B* **2003**, *41*, 97−114.

(3) Pannov, G. I.; Sobolev, V. I.; Kharitonov, A. S. The role of iron in N_2O decomposition on ZSM-5 zeolite and reactivity of the surface oxygen formed. *J. Mol. Catal.* **1990**, *61*, 85−97.

(4) Panov, G. I.; Starokon, E. V.; Ivanov, D. P.; Pirutko, L. V.; Kharitonov, A. S. Active and super active oxygen on metals in comparison with metal oxides. *Catal. Rev.: Sci. Eng.* **2021**, *63*, 597−638.

(5) Dubkov, K. A.; Paukshtis, E. A.; Panov, G. I. Stoichiometry of oxidation reactions involving alpha-oxygen on FeZSM-5 zeolite. *Kinet. Catal.* **2001**, *42*, 205−211.

(6) Ivanov, D. P.; Sobolev, V. I.; Panov, G. I. Deactivation by coking and regeneration of zeolite catalysts for benzene-to-phenol oxidation. *Appl. Catal., A* **2003**, *241*, 113−121.
(7) Dubkov, K. A.; Sobolev, V. I.; Panov, G. I. Low-temperature oxidation of methane to methanol on FeZSM-5 zeolite. *Kinet. Catal.* **1998**, *39*, 72−79.
(8) Sklenak, S.; Andrikopoulos, P. C.; Boekfa, B.; Jansang, B.; Nováková, J.; Benco, L.; Bucko, T.; Hafner, J.; Dědeček, J.; Sobalík, Z. N_2O decomposition over Fe-zeolites: Structure of the active sites and the origin of the distinct reactivity of Fe-ferrierite, Fe-ZSM-5, and Fe-beta. A combined periodic DFT and multispectral study. *J. Catal.* **2010**, *272*, 262−274.
(9) Snyder, B. E. R.; Vanelderen, P.; Bols, M. L.; Hallaert, S. D.; Böttger, L. H.; Ungur, L.; Pierloot, K.; Schoonheydt, R. A.; Sels, B. F.; Solomon, E. I. The active site of low-temperature methane hydroxylation in iron-containing zeolites. *Nature* **2016**, *536*, 317−321.
(10) Tabor, E.; Lemishka, M.; Sobalik, Z.; Mlekodaj, K.; Andrikopoulos, P. C.; Dedecek, J.; Sklenak, S. Low-temperature selective oxidation of methane over distant binuclear cationic centers in zeolites. *Commun. Chem.* **2019**, *2*, 71.
(11) Tabor, E.; Dedecek, J.; Mlekodaj, K.; Sobalik, Z.; Andrikopoulos, P. C.; Sklenak, S. Dioxygen dissociation over man-made system at room temperature to form the active alpha-oxygen for methane oxidation. *Sci. Adv.* **2020**, *6*, eaaz9776.
(12) Yuan, S.; Li, Y. D.; Peng, J. Y.; Questell-Santiago, Y. M.; Akkiraju, K.; Giordano, L.; Zheng, D. J.; Bagi, S.; Román-Leshkov, Y.; Shao-Horn, Y. Conversion of methane into liquid fuels-bridging thermal catalysis with electrocatalysis. *Adv. Energy Mater.* **2020**, *10*, 2002154.
(13) Tabor, E.; Lemishka, M.; Olszowka, J. E.; Mlekodaj, K.; Dedecek, J.; Andrikopoulos, P. C.; Sklenak, S. Splitting dioxygen over distant binuclear Fe sites in zeolites. Effect of the local arrangement and framework topology. *ACS Catal.* **2021**, *11*, 2340−2355.
(14) Dedecek, J.; Tabor, E.; Andrikopoulos, P. C.; Sklenak, S. Splitting dioxygen over distant binuclear transition metal cationic sites in zeolites. Effect of the transition metal cation. *Int. J. Quantum Chem.* **2021**, *121*, e26611.
(15) Mlekodaj, K.; Lemishka, M.; Sklenak, S.; Dedecek, J.; Tabor, E. Dioxygen splitting at room temperature over distant binuclear transition metal centers in zeolites for direct oxidation of methane to methanol. *Chem. Commun.* **2021**, *57*, 3472−3475.
(16) Dedecek, J.; Lucero, M. J.; Li, C. B.; Gao, F.; Klein, P.; Urbanova, M.; Tvaruzkova, Z.; Sazama, P.; Sklenak, S. Complex analysis of the aluminum siting in the framework of silicon-rich zeolites. A case study on ferrierites. *J. Phys. Chem. C* **2011**, *115*, 11056−11064.
(17) Andrikopoulos, P. C.; Sobalik, Z.; Novakova, J.; Sazama, P.; Sklenak, S. Mechanism of framework oxygen exchange in Fe-zeolites: A combined DFT and mass spectrometry study. *ChemPhysChem* **2013**, *14*, 520−531.
(18) Sklenak, S.; Andrikopoulos, P. C.; Whittleton, S. R.; Jirglova, H.; Sazama, P.; Benco, L.; Bucko, T.; Hafner, J.; Sobalik, Z. Effect of the Al siting on the structure of Co(II) and Cu(II) cationic sites in ferrierite. A periodic DFT molecular dynamics and FTIR study. *J. Phys. Chem. C* **2013**, *117*, 3958−3968.
(19) Kresse, G.; Hafner, J. Ab-initio molecular-dynamics for open-shell transition-metals. *Phys. Rev. B* **1993**, *48*, 13115−13118.
(20) Kresse, G.; Hafner, J. Ab-initio molecular-dynamics simulation of the liquid-metal amorphous-semiconductor transition in germanium. *Phys. Rev. B* **1994**, *49*, 14251−14269.
(21) Kresse, G.; Furthmüller, J. Efficient iterative schemes for ab initio total-energy calculations using a plane-wave basis set. *Phys. Rev. B* **1996**, *54*, 11169−11186.
(22) Kresse, G.; Furthmüller, J. Efficiency of ab-initio total energy calculations for metals and semiconductors using a plane-wave basis set. *Comput. Mater. Sci.* **1996**, *6*, 15−50.
(23) Benco, L.; Bucko, T.; Grybos, R.; Hafner, J.; Sobalik, Z.; Dedecek, J.; Hrusak, J. Adsorption of NO in Fe^{2+}-exchanged ferrierite. A density functional theory study. *J. Phys. Chem. C* **2007**, *111*, 586−595.
(24) Benco, L.; Bucko, T.; Grybos, R.; Hafner, J.; Sobalik, Z.; Dedecek, J.; Sklenak, S.; Hrusak, J. Multiple adsorption of NO on Fe^{2+} cations in the alpha- and beta-positions of ferrierite: An experimental and density functional study. *J. Phys. Chem. C* **2007**, *111*, 9393−9402.
(25) Blöchl, P. E. Projector augmented-wave method. *Phys. Rev. B* **1994**, *50*, 17953−17979.
(26) Kresse, G.; Joubert, D. From ultrasoft pseudopotentials to the projector augmented-wave method. *Phys. Rev. B* **1999**, *59*, 1758−1775.
(27) Perdew, J. P.; Burke, K.; Ernzerhof, M. Generalized gradient approximation made simple. *Phys. Rev. Lett.* **1996**, *77*, 3865−3868.
(28) Steinmann, S. N.; Corminboeuf, C. Comprehensive bench marking of a density-dependent dispersion correction. *J. Chem. Theory Comput.* **2011**, *7*, 3567−3577.
(29) Steinmann, S. N.; Corminboeuf, C. A generalized-gradient approximation exchange hole model for dispersion coefficients. *J. Chem. Phys.* **2011**, *134*, 044117.
(30) Carreón-Macedo, J. L.; Harvey, J. N. Computational study of the energetics of $^3Fe(CO)_4$, $^1Fe(CO)_4$ and $^1Fe(CO)_4(L)$, L = Xe, CH_4, H_2 and CO. *Phys. Chem. Chem. Phys.* **2006**, *8*, 93−100.
(31) Tabor, E.; Mlekodaj, K.; Sádovská, G.; Bernauer, M.; Klein, P.; Sazama, P.; Dědeček, J.; Sobalík, Z. Structural stability of metal containing ferrierite under the conditions of HT-N_2O decomposition. *Microporous Mesoporous Mater.* **2019**, *281*, 15−22.
(32) Tabor, E.; Sádovská, G.; Bernauer, M.; Sazama, P.; Nováková, J.; Fíla, V.; Kmječ, T.; Kohout, J.; Závěta, K.; Sobalík, Z. Feasibility of application of iron zeolites for high-temperature decomposition of N_2O under real conditions of the technology for nitric acid production. *Appl. Catal., B* **2019**, *240*, 358−366.
(33) Starokon, E. V.; Parfenov, M. V.; Pirutko, L. V.; Abornev, S. I.; Panov, G. I. Room-temperature oxidation of methane by alpha-oxygen and extraction of products from the FeZSM-5 surface. *J. Phys. Chem. C* **2011**, *115*, 2155−2161.
(34) Starokon, E. V.; Parfenov, M. V.; Arzumanov, S. S.; Pirutko, L. V.; Stepanov, A. G.; Panov, G. I. Oxidation of methane to methanol on the surface of FeZSM-5 zeolite. *J. Catal.* **2013**, *300*, 47−54.
(35) Parfenov, M. V.; Starokon, E. V.; Pirutko, L. V.; Panov, G. I. Quasicatalytic and catalytic oxidation of methane to methanol by nitrous oxide over FeZSM-5 zeolite. *J. Catal.* **2014**, *318*, 14−21.
(36) Göltl, F.; Michel, C.; Andrikopoulos, P. C.; Love, A. M.; Hafner, J.; Hermans, I.; Sautet, P. Computationally exploring confinement effects in the methane-to-methanol conversion over iron-oxo centers in zeolites. *ACS Catal.* **2016**, *6*, 8404−8409.
(37) Snyder, B. E. R.; Bols, M. L.; Rhoda, H. M.; Plessers, D.; Schoonheydt, R. A.; Sels, B. F.; Solomon, E. I. Cage effects control the mechanism of methane hydroxylation in zeolites. *Science* **2021**, *373*, 327−331.

https://doi.org/10.1021/acs.jpcc.1c10821
J. Phys. Chem. C 2022, 126, 4854−4861